JOURNAL OF SOLID STATE CHEMISTRY 64, 67–75 (1986)

Heat Capacity Anomalies Due to the Cooperative Jahn-Teller Effect in $Cu_{1-x}Ni_xCr_2O_4$

HIDEAKI INABA, HARUYOSHI YAGI, AND KEIJI NAITO

Department of Nuclear Engineering, Faculty of Engineering, Nagoya University, Furo-cho, Chikusa-ku, Nagoya 464, Japan

Received September 18, 1985

Heat capacities of $Cu_{1-x}Ni_xCr_2O_4$ were measured for various x values, $x = 0.0, 0.2, 0.5, 0.7, 0.85$, and 1.0, in the temperature range 220 to 960 K. The heat capacity anomalies due to the cubic-tetragonal transition resulting from the cooperative Jahn-Teller effect were observed in all the samples and that due to the tetragonal-orthorhombic transition was observed in $Cu_{0.15}Ni_{0.85}Cr_2O_4$. The excess heat capacities due to the cubic-tetragonal transition were obtained from the cooperative part of the heat capacity curves, of which shapes were similar as those obtained from the theoretical calculation proposed by Kataoka and Kanamori. The enthalpy and entropy changes due to the cubic-tetragonal transition were obtained as 6.38, 5.47, 2.34, 1.21, and 0.89 kJ mol^{-1} and 8.69, 7.99, 4.29, 2.86, and 2.59 J K^{-1} mol^{-1} for $Cu_{1-x}Ni_xCr_2O_4$ with x values of 0.0, 0.2, 0.5, 0.7, and 0.85, respectively, which are roughly in agreement with the theoretical calculation by Kataoka and Kanamori.

Introduction

Many magnetic spinel-type oxides are known to show the phase transitions (*1–10*) due to the cooperative Jahn-Teller effect as well as due to the magnetic ordering. A number of X-ray diffraction studies on chromites (*1–6*), ferrites (*7*), or manganites (*7*) have shown the structural changes of crystals due to the cooperative Jahn-Teller effect. Studies of Mössbauer spectroscopy (*6, 11*) and infrared spectroscopy (*12*) have shown the local distortions around the Jahn-Teller ions. The phase transition due to the cooperative Jahn-Teller effect has also been observed by the measurements of electrical conductivity (*4, 13*), elastic constant (*14*), and thermal expansion (*14*).

In the chromites, $CuCr_2O_4$ and $NiCr_2O_4$, the Jahn-Teller ions Cu^{2+} and Ni^{2+} enter the tetrahedral sites in the spinel structure and cause a lattice distortion by removing the triple degeneracy of the ground state. The crystal structures of $CuCr_2O_4$ (*1–3*) and $NiCr_2O_4$ (*1, 3, 4*) become tetragonal below 860 K with $c/a < 1$ and below 300 K with $c/a > 1$, respectively. In the mixed oxides, $Cu_{1-x}Ni_xCr_2O_4$, the tetragonal phases with $c/a < 1$ and $c/a > 1$, which extend from $x = 0$ and $x = 1$, are separated by a narrow region of an orthorhombic phase around $x = 0.85$ (*1, 15*).

Some theoretical attempts (*7, 16–18*) to predict the temperature dependence of the order parameter have been made by considering the free energy of the system. To understand the mechanism of the cooperative Jahn-Teller effect, it is desirable to compare the measured quantities derived from the free energy of the system—enthalpy

0022-4596/86 $3.00

and entropy changes and excess heat capacity due to the phase transition—with the theoretical ones. Since the phase transitions of these compounds have well been analyzed theoretically by Kataoka and Kanamori (*16*), we can easily compare the experimental results with the theory. However, only a few measurements of heat capacity for this purpose have been made on $Fe_{1+x}Cr_{2-x}O_4$ (*6*), $CuFe_2O_4$ (*8*), and $TmVO_4$ (*18*), mainly at low temperatures.

In this study, we have conducted the heat capacity measurement of $Cu_{1-x}Ni_xCr_2O_4$ with x values of 0.0, 0.2, 0.5, 0.7, 0.85, and 1.0 in the range 220 to 960 K.

Experimental

Sample preparation. The $CuCr_2O_4$ sample was prepared by sintering the mixture of CuO and Cr_2O_3 as follows: the same mole amounts of CuO and Cr_2O_3, both with 99.99% purity, were mixed in acetone, and sintered in air at 1273 K for 24 hr, and after mixing again in acetone, annealed in air at 1123 K for 48 hr and then cooled slowly to room temperature. Similarly, for the $NiCr_2O_4$ sample, the same mole amounts of NiO and Cr_2O_3 (99.99% purity) were mixed in acetone and sintered in air at 1653 K for 72 hr, and after mixing again in acetone, annealed in air for 48 hr and then cooled slowly to room temperature. For the mixed oxides, $Cu_{1-x}Ni_xCr_2O_4$, the samples $CuCr_2O_4$ and $NiCr_2O_4$ thus obtained were mixed in a proper ratio and sintered in air at 1273 K for 48 hr, and after mixing again, annealed in air at 1273 K for 48 hr, kept at 1023 K for 48 hr, and then slowly cooled to room temperature.

The X-ray diffraction pattern of $Cu_{1-x}Ni_xCr_2O_4$ except $x = 0.85$ was taken at room temperature by Debye–Sherrer camera, showing the single phase of tetragonal symmetry. In the case of $Cu_{0.15}Ni_{0.85}Cr_2O_4$, the orthorhombic lattice constants were calculated from the three diffraction lines corresponding (311), (131), and (113). The results were in good agreement with those reported by Wold *et al.* (*15*).

Heat capacity measurement. Heat capacity of $Cu_{1-x}Ni_xCr_2O_4$ was measured by an adiabatic scanning calorimeter (*20*), where the power supplied to the sample was measured continuously, and the heating rate was kept constant regardless of the kind and amount of the sample. The heating rate chosen was 2 K min^{-1}, and the measurement was carried out between 220 to 960 K under nitrogen gas at about 400 Pa. The variations in the heating rate and in the adiabatic control were maintained within 0.01 K min^{-1} and 0.01 K, respectively. The $Cu_{1-x}Ni_xCr_2O_4$ sample powder was sealed in a quartz vessel filled with helium gas at about 16 kPa. The amount used for the measurement was about 14 g for each sample.

Results

The results of the heat capacity measurement on $Cu_{1-x}Ni_xCr_2O_4$ for x values of 0.0, 0.2, 0.5, 0.7, 0.85, and 1.0 are shown in Figs. 1, 2, and 3. The heat capacity anomalies due to the cooperative Jahn-Teller effect are seen in the figures. These anomalies become smaller and shift to lower temperatures as x increases. The noncooperative part of the heat capacities is estimated by connecting the baselines of heat capacity curves smoothly as shown by broken lines in Figs. 1–3. Using these baselines, the cooperative part of heat capacities for $Cu_{1-x}Ni_xCr_2O_4$ is calculated and examples for $Cu_{0.8}Ni_{0.2}Cr_2O_4$ and $Cu_{0.5}Ni_{0.5}Cr_2O_4$ are shown in Figs. 4 and 5. The transition temperatures, enthalpy and entropy changes due to the transition are obtained from the cooperative parts of the heat capacity and the results are listed in Table I and are shown in Figs. 6, 7, and 8, respec-

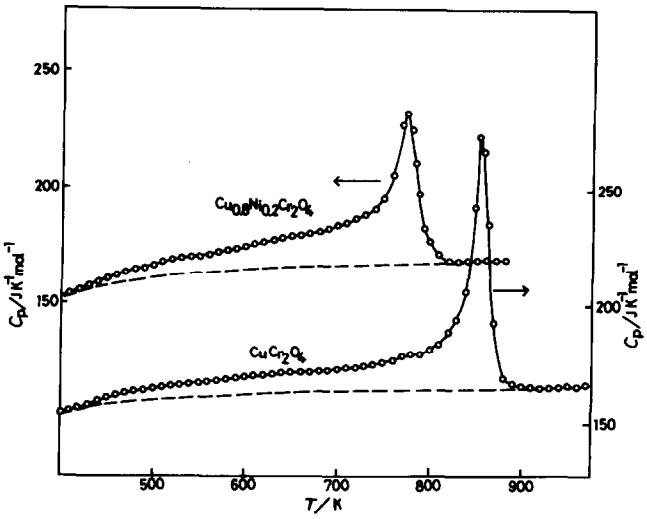

FIG. 1. Heat capacities of $CuCr_2O_4$ and $Cu_{0.8}Ni_{0.2}Cr_2O_4$. The left ordinate is for $Cu_{0.8}Ni_{0.2}Cr_2O_4$ and the right ordinate is for $CuCr_2O_4$. The broken lines show the noncooperative heat capacities.

tively. In Fig. 6, the transition temperatures obtained by X-ray diffractometry (*1*) are also shown for comparison. The agreement between the results obtained by the two different methods is satisfactory.

Discussion

Statistical Model for the Cooperative Jahn-Teller Distortion

The statistical models of the spontaneous

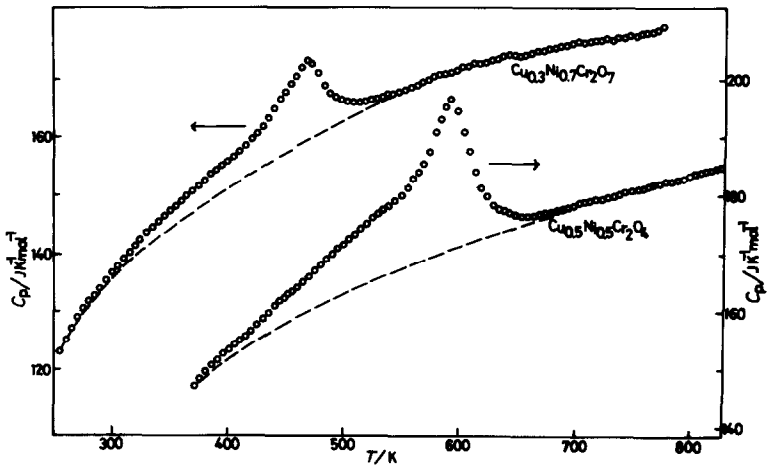

FIG. 2. Heat capacities of $Cu_{0.5}Ni_{0.5}Cr_2O_4$ and $Cu_{0.3}Ni_{0.7}Cr_2O_4$. The left ordinate is for $Cu_{0.3}Ni_{0.7}Cr_2O_4$ and the right ordinate is for $Cu_{0.5}Ni_{0.5}Cr_2O_4$. The broken lines show the noncooperative heat capacities.

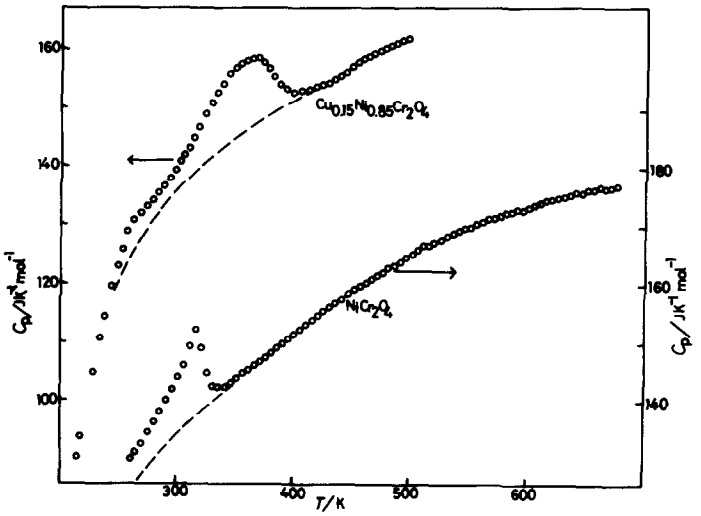

FIG. 3. Heat capacities of $Cu_{0.15}Ni_{0.85}Cr_2O_4$ and $NiCr_2O_4$. The left ordinate is for $Cu_{0.15}Ni_{0.85}Cr_2O_4$ and the right ordinate is for $NiCr_2O_4$. The broken lines show the noncooperative heat capacities.

crystal distortion were proposed by Finch *et al.* (*7*) and Wojtowicz (*17*) on the basis of the assumption that the phenomenon was the cooperative alignment of the local distortions associated with the Jahn-Teller ions. In the former case (*7*), being applied to $CuFe_2O_4$, a local distortion, tetragonally distorted octahedron, is assumed to lower

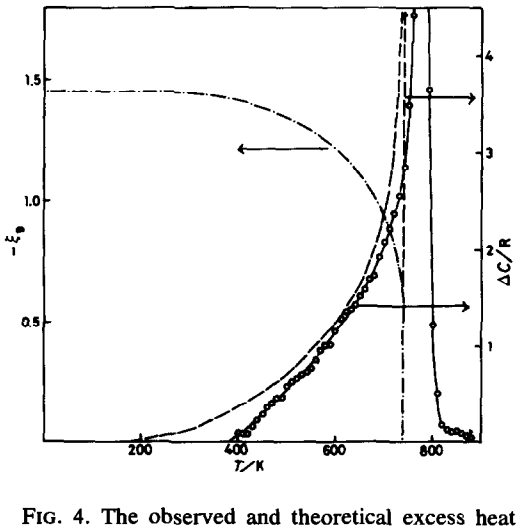

FIG. 4. The observed and theoretical excess heat capacities and the theoretical order parameter as a function of temperature for $Cu_{0.8}Ni_{0.2}Cr_2O_4$. O, Observed excess heat capacity; ——, theoretical heat capacity; ·—·—, theoretical order parameter.

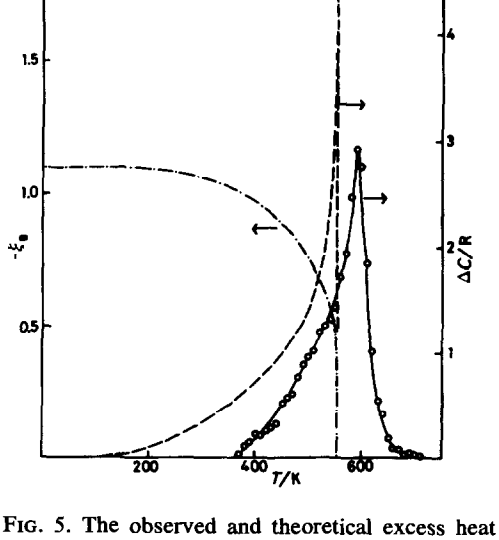

FIG. 5. The observed and theoretical excess heat capacities and the theoretical order parameter as a function of temperature for $Cu_{0.5}Ni_{0.5}Cr_2O_4$. O, Observed excess heat capacity; ——, theoretical excess heat capacity; ·—·—, theoretical order parameter.

TABLE I

THE CALCULATED AND OBSERVED RESULTS OF TRANSITION TEMPERATURES (t_{c2}), ENTHALPY CHANGE (ΔH), AND ENTROPY CHANGE (ΔS) DUE TO THE CUBIC-TETRAGONAL TRANSITION FOR $Cu_{1-x}Ni_xCr_2O_4$

Sample: x in $Cu_{1-x}Ni_xCr_2O_4$	t_{c2} (K)		ΔH (kJ mol^{-1})		ΔS (J K^{-1} mol^{-1})	
	Calculated	Observed	Calculated	Observed	Calculated	Observed
0.0	865	862	6.74	6.38	9.13	8.69
0.2	741	768	4.96	5.47	7.98	7.99
0.5	556	590	2.77	2.34	6.07	4.29
0.7	437	469	1.39	1.21	3.52	2.86
0.85	354	355	0.26	0.89	0.63	2.59
1.00	302	309	2.35	—	9.13	—

the energy of the system by W, if the direction of the local distortion is the same as that of the crystal, and the distortion parameter $\sigma(\equiv c/a - 1)$ is represented by

$$\sigma/\sigma_e = \tanh(W/kT) = \tanh[(T_c/T)(\sigma/\sigma_e)], \quad (1)$$

where σ_e is the distortion parameter of each distorted octahedron and T_c is the transition temperature. Equation (1) is the same as that by Bragg and Williams (*21*) applied to the order–disorder transition in binary alloys. In the latter case (*17*), the free energy of the system $F(\sigma)$ is obtained by assuming the pair interactions between the nearest-neighboring octahedra as

$$F(\sigma) - F(0) = 2/3RT(1 + 2\sigma)\ln(1 + 2\sigma) + 2(1 - \sigma)\ln(1 - \sigma) - \sigma^2/J, \quad (2)$$

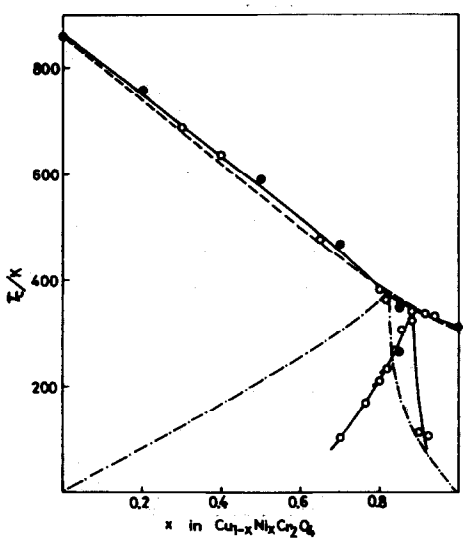

FIG. 6. Transition temperatures of $Cu_{1-x}Ni_xCr_2O_4$. ○, Kino and Miyahara by X-ray diffractometry; ●, present results; ——, theoretical calculation (cubic-tetragonal); ·—·—, theoretical calculation (tetragonal-orthorhombic).

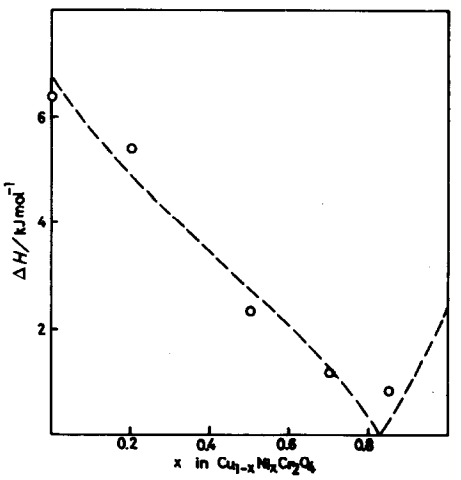

FIG. 7. Enthalpy change due to the cubic-tetragonal transition as a function of composition. ○, Observed; ——, theoretical.

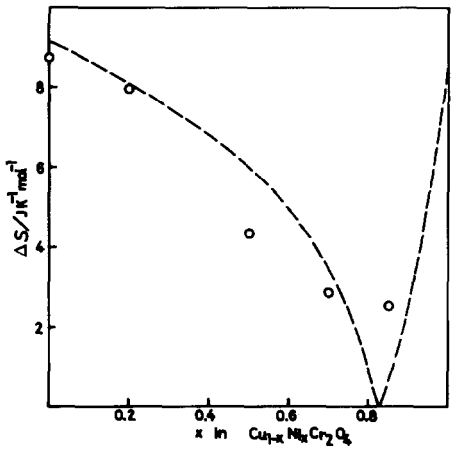

FIG. 8. Entropy change due to the cubic-tetragonal transition as a function of composition. O, Observed; ---, theoretical.

$$F(0) = E(0) - 2RT \ln 3, \quad (3)$$

where σ is the order parameter, J is the reduced temperature, and $E(0)$ is the configurational energy of the cubic phase at $\sigma = 0$. These two models, however, were rather phenomenological.

The model using a microsopic Hamiltonian was proposed by Kanamori (*18*), and it was refined by Kataoka and Kanamori (*16*). In the model by Kataoka and Kanamori (*16*), the bulk distortions of mixed crystals are assumed to be calculated on the basis of a Hamiltonian, which consists of the elastic energy, the energy of the lattice vibrations, the interaction between the electronic states of each ion and the uniform strains originating in the crystalline field, and the interaction between the electronic states and relative displacements.

Applying the model by Kataoka and Kanamori (*16*) to $Cu_{1-x}Ni_xCr_2O_4$, the free energy of the system, f, is represented by

$$f = \frac{C_0}{2}(u_2^2 + u_3^2) - RT\{(1-x)\ln z_{Cu} + x \ln z_{Ni}\}, \quad (4)$$

where C_0 is the renormalized elastic constant, u_2 and u_3 are the parameters for the bulk distortion derived from the linear combinations of elastic strains, e_{ij},

$$u_2 = (1/\sqrt{2})(e_{xx} - e_{yy}),$$

$$u_3 = (1/\sqrt{6})(2e_{zz} - e_{xx} - e_{yy}), \quad (5)$$

and the partition functions z_M are defined as follows:

$$z_M = \exp\{-(2/\sqrt{6})\sqrt{C_0/N}G_0(M)u_3/kT\} + 2\exp\{(1/\sqrt{6})\sqrt{C_0/N}G_0(M)u_3/kT\} \times \cosh\{(1/\sqrt{2})\sqrt{C_0/N}G_0(M)u_2/kT\}, \quad (6)$$

where N is the Avogadro number, $G_0(M)$ is the renormalized coupling constant for Cu or Ni between the electronic states of each ion and uniform strains. In practice, it is convenient to introduce the reduced units for the parameter of free energy, temperature and coupling constant. Thus one defines

$$\xi_2 = u_2/(\sqrt{2N/3C_0}|G_0(\mathrm{Ni})|), \quad (7)$$

$$\xi_3 = u_3/(\sqrt{2N/3C_0}|G_0(\mathrm{Ni})|), \quad (8)$$

$$F = f/[\{G_0(\mathrm{Ni})\}^2/3], \quad (9)$$

$$t = kT/[\{G_0(\mathrm{Ni})\}^2/3], \quad (10)$$

and

$$r = |G_0(\mathrm{Cu})/G_0(\mathrm{Ni})|. \quad (11)$$

Then the free energy in the reduced unit, F, is represented by

$$F/N = \xi_2^2 + \xi_3^2 - t\{(1-x)\ln z_{Cu} + x \ln z_{Ni}\}, \quad (12)$$

$$z_{Cu} = \exp(-2r\xi_3/t) + 2\exp(r\xi_3/t)\cosh(\sqrt{3}r\xi_2/t) \quad (13)$$

$$z_{Ni} = \exp(2\xi_3/t) + 2\exp(-\xi_3/t)\cosh(\sqrt{3}\xi_2/t). \quad (14)$$

From the conditions for the free energy to be minimum

$$\frac{\partial(F/N)}{\partial\xi_2} = \frac{\partial(F/N)}{\partial\xi_3} = 0, \tag{15}$$

the following three solutions can be obtained.

$$\text{(i)}\quad \xi_2 = \xi_3 = 0. \tag{16}$$

$$\text{(ii)}\quad \xi_2 = 0,$$

$$\xi_3 = x\frac{\exp(3\xi_3/t) - 1}{\exp(3\xi_3/t) + 2} + r(1-x)\frac{1 - \exp(-3r\xi_3/t)}{\exp(-3\xi_3/t) + 2}. \tag{17}$$

$$\text{(iii)}\quad \xi_2 = 3r(1-x) \times \frac{\sinh(\sqrt{3}r\xi_2/t)}{\exp(-3r\xi_3/t) + 2\cosh(\sqrt{3}r\xi_2/t)} + 3x\frac{\sinh(\sqrt{3}r\xi_2/t)}{\exp(3\xi_3/t) + 2\cosh(\sqrt{3}\xi_2/t)},$$

$$\xi_3 = x\frac{\exp(3\xi_3/t) - \cosh(\sqrt{3}\xi_2/t)}{\exp(3\xi_3/t) + 2\cosh(\sqrt{3}\xi_2/t)} + r(1-x) \times \frac{\cosh(\sqrt{3}r\xi_2/t) - \exp(-3r\xi_3/t)}{\exp(-3r\xi_3/t) + 2\cosh(\sqrt{3}r\xi_2/t)}. \tag{18}$$

Equations (16), (17), and (18) give the parameters of distortion ξ_2 and ξ_3 at a given temperature in the cubic, tetragonal, and orthorhombic phases, respectively.

Transition Temperatures

At the cubic-tetragonal transition temperature (t_{c2}), the relation:

$$\left(\frac{\partial^2\{F/N\}}{\partial\xi_3^2}\right)_{\xi_3=0} = \left(\frac{\partial^2\{F/N\}}{\partial\xi_3^2}\right)_{\xi_3\neq 0} = 0 \tag{19}$$

holds. And then

$$9r^2(1-x) \times \frac{\exp(-r\xi_3/t_{c2})}{\{\exp(-2r\xi_3/t_{c2}) + 2\exp(r\xi_3/t_{c2})\}^2} + 9x\frac{\exp(\xi_3/t_{c2})}{\{\exp(2\xi_3/t_{c2}) + 2\exp(-\xi_3/t_{c2})\}^2} = r^2(1-x) + x \tag{20}$$

is obtained. The values for t_{c2} ($x = 1.0$) and t_{c2} ($x = 0$), 1.082 and 1.082 r^2 are, respectively, obtained from Eq. (20). Using the experimental transition temperatures (l) for $x = 1.0$ (300 K) and $x = 0.0$ (860 K), r is obtained to be 1.69, and using Eq. (10) t is represented by $0.0036067T$. Using Eq. (17) and these values for r and t thus obtained, the temperature of the cubic-tetragonal transition for each intermediate composition is obtained by a numerical calculation on condition that ξ_3 at the minimum free energy becomes zero. The results are listed in Table I and shown as a broken curve in Fig. 6. It is noted from the figure that the agreement between the two experimental results (the present results and those of Ref. (*1*)) and the theoretical values are considered to be good, although the theoretical transition temperatures are slightly lower than the experimental ones in the region $x < 0.7$.

At the tetragonal-orthorhombic transition temperature (t_{c1}),

$$\left(\frac{\partial^2\{F/N\}}{\partial\xi_2^2}\right)_{\xi_2=0} = 0, \tag{21}$$

holds. And then

$$t_{c1} = \frac{3r^2(1-x)}{\exp(-3r\xi_3/t_{c1}) + 2} + \frac{3x}{\exp(3\xi_3/t_{c1}) + 2}, \tag{22}$$

is obtained. Using Eqs. (17) and (22), t_{c1} for various x values can be obtained and the results are shown as chain lines in Fig. 6. The present results of t_{c1} obtained in the present study for $Cu_{0.15}Ni_{0.85}Cr_2O_4$ are in good agreement with those by Kino and

Miyahara (*1*), but the theoretical values of t_{c1} shift considerably to the lower composition side as seen in Fig. 6.

Excess Heat Capacity, Enthalpy Change, and Entropy Change Due to the Phase Transition

Since Kataoka and Kanamori (*16*) did not derive the excess heat capacity, enthalpy and entropy changes due to the phase transition in explicit form, we derive them here in order to compare them with the experimental results. Putting $\xi_2 = 0$ in Eq. (12), the entropy at t becomes

$$S(t) = -\left(\frac{\partial\{F/N\}}{\partial t}\right) = (1-x)\ln\{\exp(-2r\xi_3/t) + 2\exp(r\xi_3/t)\} + x\ln\{\exp(2\xi_3/t) + 2\exp(-\xi_3/t)\} - 2\xi_3^2/t. \quad (23)$$

The entropy change of the cubic-tetragonal transition ΔS is represented by

$$\Delta S = S(\xi_3 = 0) - S(t_{c1}). \quad (24)$$

Using Eqs. (17) and (23) the excess heat capacity due to the cubic-tetragonal transition ΔC is represented by

$$\Delta C = t\left(\frac{\partial S(t)}{\partial t}\right) = -2\xi_3\frac{\partial \xi 3}{\partial t} = -18\xi_3^2 B/A, \quad (25)$$

where $A = 9r^2(1-x)D/t(D+2)^2 + 9xE/t(E+2)^2 - 1$, $B = r^2(1-x)D/t^2(D+2)^2 + xE/t^2(E+2)^2$, $D = \exp(-3r\xi_3/t)$ and $E = \exp(3\xi_3/t)$.

The calculated ΔC and ξ_3 for $Cu_{0.8}Ni_{0.2}Cr_2O_4$ and $Cu_{0.5}Ni_{0.5}Cr_2O_4$ are shown in Figs. 4 and 5, respectively, together with the observed excess heat capacities. The order parameter ξ_3 is negative ($u_3 < 0$) in the region $0 \leqq x \lesssim 0.82$, where $c/a < 1$. Though the transition temperatures are different between the observed and theoretical results, the behaviors of the excess heat capacities below the transition temperatures are quite similar in both results. As seen from the order parameter ξ_3 and ΔC at the transition temperatures in Figs. 4 and 5, the cubic-tetragonal transition should theoretically be first order. Owing to the dynamic character of the calorimeter (*20*), however, the finite rather than infinite heat capacities are observed as seen in Figs. 1–3 and 5. It is, therefore, not possible experimentally to determine whether these transitions are first order or not. Considerable amounts of the excess heat capacities above the transition temperatures are observed experimentally as seen in Figs. 4 and 5, which show the existence of the short-range ordering above the transition temperatures.

The enthalpy change ΔH due to the cubic-tetragonal transition is calculated as

$$\Delta H = \int_{t_{c1}}^{t_{c2}} \Delta C dt + t_{c2}\{S(\xi_3 = 0) - S(t_{c2})\}. \quad (26)$$

The calculated entropy and enthalpy changes due to the transition for various x values are obtained according to Eqs. (24) and (26) and the results are shown in Table I and in Figs. 7 and 8 together with the experimental results. The agreement between the observed and the theoretical results is fairly good, considering the error in determining the baseline heat capacities shown in Figs. 1–3 and the error based on the assumptions made in the theoretical calculation (*16*).

References

1. Y. Kino and S. Miyahara, *J. Phys. Soc. Japan* **21,** 2732 (1966).
2. S. Miyahara and H. Ohnishi, *J. Phys. Soc. Japan* **12,** 1296 (1956).
3. G. Kim, J. Sakurai, and Y. Komura, *Japan. J. Appl. Phys.* **15,** 411 (1976).
4. P. Pausescu and R. Manaila, *Sov. Phys.-Cryst.* **13,** 533 (1969).
5. T. Kubo, *J. Phys. Soc. Japan* **28,** 430 (1970).
6. K. Kose and S. Iida, *J. Appl. Phys.* **55,** 2321 (1981).

7. G. I. FINCH, A. P. B. SINHA, AND K. P. SINHA, *Proc. R. Soc. London Ser. A* **242,** 28 (1957).
8. T. INOYE AND S. IIDA, *J. Phys. Soc. Japan* **13,** 656 (1958).
9. K. NAITO, H. INABA, AND H. YAGI, *J. Solid State Chem.* **36,** 28 (1981).
10. H. INABA, S. NAKASHIMA, AND K. NAITO, *J. Solid State Chem.* **41,** 213 (1982).
11. M. TANAKA, T. TOKORO, AND Y. AIYAMA, *J. Phys. Soc. Japan* **21,** 262 (1966).
12. J. SIRATORI AND Y. AIYAMA, *J. Phys. Soc. Japan* **20,** 1962 (1965).
13. M. ROSENBERG, P. NICOLAU, R. MANAILA, AND P. PAUSESCU, *J. Phys. Chem. Solids* **24,** 1419 (1963).
14. Y. KINO, B. LUTHI, AND M. E. MULLEN, *J. Phys. Soc. Japan* **33,** 687 (1972).
15. A. WOLD, R. J. ARNOTT, E. WHIPPLE, AND J. B. GOODENOUGH, *J. Apply. Phys.* **34,** 1085 (1963).
16. M. KATAOKA AND J. KANAMORI, *J. Phys. Soc. Japan* **32,** 113 (1972).
17. P. J. WOJTOWICZ, *Phys. Rev.* **19,** 32 (1959).
18. J. KANAMORI, *J. Appl. Phys.* **31,** 145 (1960).
19. A. H. COOKE, S. T. SWITHEMBY, AND M. R. WELLS, *Solid State Commun.* **10,** 265 (1972).
20. K. NAITO, H. INABA, M. ISHIDA, Y. SAITO, AND H. ARIMA, *J. Phys. E* **7,** 464 (1974).
21. W. L. BRAGG AND E. J. WILLIAMS, *Proc. R. Soc. London Ser. A* **151,** 540 (1935).